

X-ray diffraction: Tube measurements were done at room temperature on a Bruker SMART CCD diffractometer ($\text{MoK}\alpha$). Data collection and integration was carried out with the SMART software. Averaging and empirical absorption corrections were carried out with SADABS.^[10] Least-squares refinements were made with programs LINEX^[11] and XD^[12] in the space group $Pm\bar{3}n$. For both structures free refinement of framework atom occupancies resulted in random distributions of Ga and Ge atoms. Refinement of guest atoms occupancies showed all sites to be fully occupied except Sr(1), which refined to 98.6(4) % occupancy. In both refinements anisotropic thermal parameters were employed on all atoms as well as isotropic extinction parameters. For $\text{Sr}_8\text{Ga}_{16}\text{Ge}_{30}$ a split-atom model was used for Sr(2) as in reference [6] ($(x, y, z) = (0, 0.4784, 0.9784)$). $\text{Sr}_8\text{Ga}_{16}\text{Ge}_{30}$ [$\text{Ba}_8\text{Ga}_{16}\text{Ge}_{30}$]: $a = 10.740(2)$ [10.785(2)] Å, $V = 1238.7(1)$ [1254.4(1)] Å³, $V_{\text{crystal}} = 0.0004$ [0.0003] mm³, $\rho_{\text{calcd}} = 5.354$ [5.791] g cm⁻³, $\lambda = 0.7107$ Å, $(\sin\theta/\lambda)_{\text{max}} = 0.923$ [0.836] Å⁻¹, $\mu_1 = 345$ [322] cm⁻¹, T_{max} , $T_{\text{min}} = 0.2060, 0.0883$ [0.2534, 0.1132], no. of measured reflections = 35927 [54576], no. of unique = 691 [558], $R_{\text{w}}(\text{int}) = 0.0451$ [0.0361], $N_{\text{obs}} = 691$ [558] ($I > 0\sigma(I)$), $N_{\text{par}} = 19$ [16], $\text{GOF} = 0.40$ [0.52], $R_{\text{F}} = 0.0256$ [0.0170], $R_{\text{wF}} = 0.0254$ [0.0169], $Y_{\text{min}}(\text{extinction}) = 0.79$ [0.81] (10 and 8 reflections have $Y < 0.95$). Further details on the crystal structure investigations may be obtained from the Fachinformationszentrum Karlsruhe, 76344 Eggenstein-Leopoldshafen, Germany (fax: (+49) 7247-808-666, on quoting the depository numbers CSD-411062 ($\text{Sr}_8\text{Ga}_{16}\text{Ge}_{30}$) and CSD-411063 ($\text{Ba}_8\text{Ga}_{16}\text{Ge}_{30}$)).

MEM calculations: Absorption, extinction, and anomalous dispersion-corrected observed structure factors phased and scaled with program XD were used for MEM calculations with the MEED program.^[13] The calculations employed nonuniform prior densities obtained by a structure factor aliasing procedure^[14] proposed by Roversi et al.^[15] This method is superior to straightforward Fourier transformation, which gives series termination ripples. In the present calculations 28 structure factor copies were used with a cut-off value of 10^{-9} . The nonuniform priors correspond to the EDs of assemblies of neutral atoms having anisotropic harmonic thermal motion. This means that the observed data are used to estimate the effects of chemical bonding, charge transfer, and disorder. For $\text{Sr}_8\text{Ga}_{16}\text{Ge}_{30}$ the MEM density was almost unchanged between calculations with nonuniform priors having ordered and disordered (i.e. split) Sr(2) sites. In all MEM calculations a $128 \times 128 \times 128$ pixel grid was used and iterations were stopped at $\chi^2 = 1$. Estimated standard uncertainties on the structure factors were obtained from the data averaging procedure.

Received: December 21, 1999

Revised: August 3, 2000 [Z14432]

- [1] F. J. DiSalvo, *Science* **1999**, 285, 703–706.
- [2] a) J. S. Kasper, P. Hagenmuller, M. Pouchard, *Science* **1965**, 150, 1713–1714; b) v. H. Menke, H. G. von Schnering, *Z. Anorg. Allg. Chem.* **1973**, 395, 223–238; c) B. Eisenmann, H. Schäfer, R. Zagler, *J. Less-Comm. Met.* **1986**, 118, 43–55.
- [3] B. C. Sales, B. C. Chakoumakos, D. Mandrus, J. W. Sharp, *J. Solid State. Chem.* **1999**, 146, 528–532.
- [4] The thermoelectric figure of merit is defined as $ZT = TS^2\sigma/\kappa$, where S is the Seebeck coefficient, σ the electrical conductivity, and κ the thermal conductivity.
- [5] N. P. Blake, L. Møllnitz, G. Kresse, H. Metiu, *J. Chem. Phys.* **1999**, 111, 3133–3144.
- [6] B. C. Chakoumakos, B. C. Sales, D. G. Mandrus, G. S. Nolas, *J. Alloys Compd.* **2000**, 296, 80–86.
- [7] P. Coppens, *X-ray charge densities and chemical bonding*, Oxford University Press, Oxford, **1997**.
- [8] The occupancy of the guest sites can only be less than 100 %, and thus partial occupancy on Sr(2) can only make the charge estimate more negative. Changing the occupancy on Sr(2) has little effect on the charge estimate, but for Sr(1) it alters the estimate significantly. However, changes in the Sr(1) occupancy also degrades the crystallographic R factors (e.g. $R(F^2) = 0.0274$ (95 %), $R(F^2) = 0.0256$ (98.6 %)).
- [9] MacXAFS3.6 Software Package, C. E. Bouldin, W. T. Elam, L. Furenli, *Physica B* **1995**, 208, 190–192.

- [10] Owing to the enormous redundancy of the data, empirical absorption corrections were found to give much better results than corrections based on approximate analytical crystal shapes.
- [11] P. Coppens, Program LINEX, Department of Chemistry, State University of New York at Buffalo, New York 14260, **1974**.
- [12] T. Koritsanszky, S. T. Howard, P. R. Mallison, Z. Su, T. Richter, N. K. Hansen, Program XD, Institute of Crystallography, Freie Universität, Berlin, Germany, **1999**. The program was locally modified to handle atoms with $Z > 36$ by Dr. Piero Macchi.
- [13] S. Kumazawa, Y. Kubota, M. Takata, M. Sakata, Y. Ishibashi, *J. Appl. Crystallogr.* **1993**, 26, 453–457.
- [14] A. Bentien, Program ASF, Department of Chemistry, University of Aarhus, 8000 Aarhus C, Denmark, **2000**.
- [15] P. Roversi, J. J. Irwin, G. Bricogne, *Acta Crystallogr. Sect. A* **1998**, 54, 971–996.
- [16] C. J. Howard, R. D. G. Jones, *Acta Crystallogr. Sect. A* **1977**, 33, 776.

Self-Assembly of Pentameric Porphyrin Light-Harvesting Antennae Complexes**

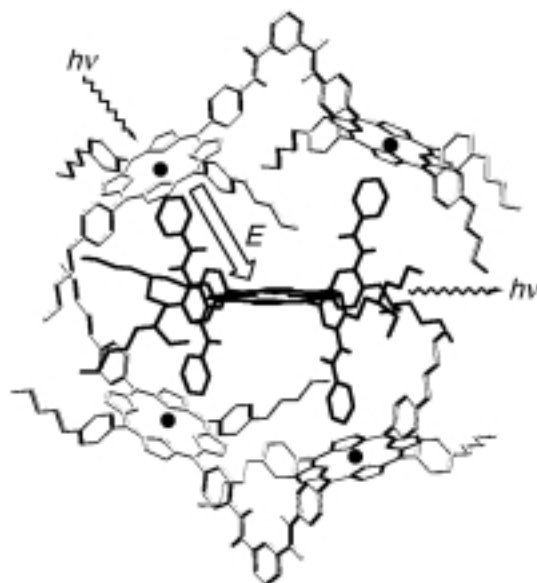
Richard A. Haycock, Arkady Yartsev,
Ulrike Michelsen, Villy Sundström, and
Christopher A. Hunter*

The reaction centers of natural photosynthetic systems are excited indirectly through their light-harvesting antennae complexes.^[1–3] These units contain a network of chromophores which absorb light energy and channel this very efficiently by singlet energy transfer to the photochemical reaction centres.^[4, 5] The photochemical properties of porphyrins lend themselves to the design of artificial organic antennae systems,^[6] and covalently linked arrays of five or more porphyrins have been constructed.^[7–10] We demonstrate here that cooperative self-assembly processes are ideally suited to the construction of stable structurally well-defined chromophore arrays for use as antennae systems.^[11, 12]

Zn₂1 and **H₂2** were designed to be perfectly complementary, preorganized partners for the self-assembly process shown in Scheme 1.^[13] Intramolecular hydrogen bonds constrain both molecules to essentially one conformation, thus minimizing the loss of rotational entropy upon binding. The spacing of the coordination sites ensures that **Zn₂1** will coordinate to the *trans-meso* ligands across the face of **H₂2** with no strain in the final complex.^[14] The central free-base porphyrin is encapsulated in a spherical array of four zinc

[*] Prof. C. A. Hunter, Dr. R. A. Haycock, Dr. U. Michelsen
Krebs Institute for Biomolecular Science
Department of Chemistry
University of Sheffield
Sheffield S3 7HF (UK)
Fax: (+44) 114-273-8673
E-mail: C.Hunter@shef.ac.uk
Dr. A. Yartsev, Prof. V. Sundström
Department of Chemistry
University of Lund
Lund (Sweden)

[**] We thank the EPSRC (R.A.H.) and the Lister Institute (C.A.H.) for funding. V.S. and A.Y. thank the Swedish NFR and the K&A Wallenberg Foundation for financial support.



A graph showing the relationship between ΔA (Y-axis) and $\text{equiv} / \text{H}_2\text{O}_2$ (X-axis). The curve is sigmoidal, starting at (0,0) and leveling off as the ratio increases. The X-axis ranges from 0.00 to 1.00 with major ticks every 0.25. The Y-axis is labeled ΔA with an upward arrow.

$\text{equiv} / \text{H}_2\text{O}_2$	ΔA (relative units)
0.00	0.00
0.05	0.15
0.10	0.25
0.15	0.35
0.20	0.45
0.25	0.55
0.30	0.65
0.35	0.72
0.40	0.78
0.45	0.82
0.50	0.85
0.55	0.87
0.60	0.88
0.65	0.89
0.70	0.90
0.75	0.91
0.80	0.92
0.85	0.92
0.90	0.93
0.95	0.93
1.00	0.93

3763

Mass spectrometric studies (ES-MS, FAB-MS, and matrix-assisted laser desorption/ionization (MALDI)) all failed to reveal the presence of complexes: only the free components could be detected in mixtures. However, vapour pressure osmometry (VPO) of a 2:1 mixture of **Zn₂1** and **H₂2** at millimolar concentrations in chloroform consistently gave a molecular weight of 7330 ± 700 , which confirmed the presence of a 2:1 complex (molecular weight = 7720). The pure components **Zn₂1** and **H₂2** do not self-associate in isolation, and give VPO molecular weights of 2890 ± 180 (**Zn₂1** = 3056) and 1640 ± 140 (**H₂2** = 1608), respectively, under the same conditions. The only structure that is consistent with all of this evidence is the porphyrin pentamer shown in Scheme 1.

The photochemical properties of the assembly were investigated using fluorescence titrations (Figure 2). **H₂** can be selectively excited at 520 nm, but it is not possible to selectively excite **Zn₁**. Emission from **H₂** can be selectively

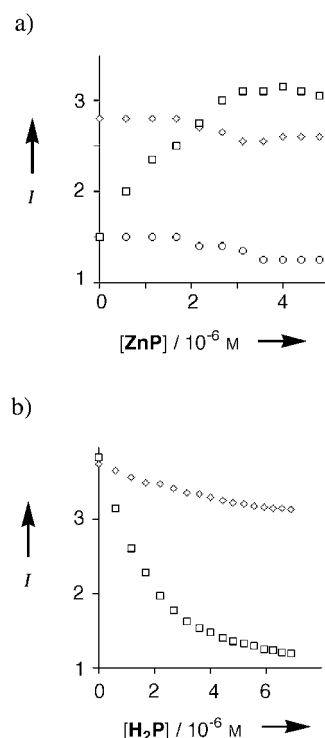
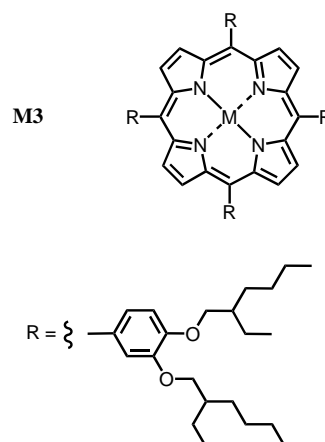


Figure 2. Fluorescence titration data in dichloromethane (fluorescence intensity I is an arbitrary scale): a) Addition of zinc porphyrins to **H₂** (2.0×10^{-6} M). \square : **ZnP** = **Zn₁**: Simultaneous excitation of both chromophores at 560 nm and emission from **H₂** at 720 nm. \diamond : **ZnP** = **Zn₂**: selective excitation of **H₂** at 520 nm and emission from **H₂** at 720 nm. \circ : **ZnP** = **Zn₃**: Simultaneous excitation of both chromophores at 560 nm and emission from **H₂** at 720 nm. b) Addition of free base porphyrins to **Zn₁**. \diamond : **H₂P** = **H₂**: Simultaneous excitation of both chromophores at 560 nm and emission from **Zn₁** at 600 nm. \square : **H₂P** = **H₂**: Simultaneous excitation of both chromophores at 560 nm and emission from **Zn₁** at 600 nm.

detected at 720 nm, and emission from **Zn₂1** can be selectively detected at 600 nm. When **Zn₂1** was added to **H₂2** and both chromophores were simultaneously excited at 560 nm, the intensity of the **H₂2** emission at 720 nm increased until two equivalents of **Zn₂1** had been added (Figure 2a). However when **H₂2** was preferentially excited at 520 nm, there was no change in the fluorescence intensity at 720 nm on addition of

Zn2.1. To prove that this behavior is a property of the complex in Scheme 1 we also investigated the titration of a monomeric zinc porphyrin which does not form stable complexes at micromolar concentrations (**Zn3**) into **H2.2**. Addition of **Zn3** caused no change in the intensity of the **H2.2** emission at



720 nm when both chromophores were simultaneously excited at 560 nm (Figure 2a). The reverse titration data are shown in Figure 2b. Addition of **H₂2** to **Zn₂1** caused a 70 % decrease in the intensity of the **Zn₂1** emission at 600 nm when both chromophores were simultaneously excited at 560 nm. When an unfunctionalized free-base porphyrin, which can not form intermolecular complexes (**H₂3**) was used in place of **H₂2**, the decrease in the intensity of the **Zn₂1** emission arising from competitive absorption was very small. We conclude therefore that the formation of the 2:1 complex in Scheme 1 quenches the **Zn₂1** fluorescence and enhances the **H₂2** emission as a result of energy transfer from the antennae zinc porphyrins to the free-base core of the complex.

Time-resolved experiments using streak-camera fluorescence measurements were undertaken to determine the rate of energy transfer (Figure 3). In pure samples, the fluorescence decay time of **Zn,1** is 1330 ± 20 ps, and the fluorescence

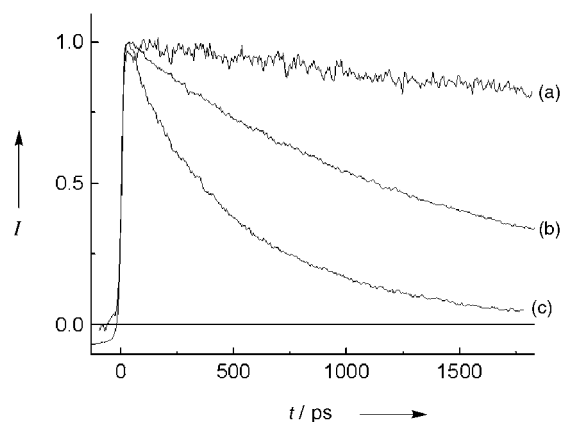


Figure 3. Fluorescence decay profiles (excitation at 562 nm) showing normalized fluorescence intensity (I) as a function of time (t): a) emission from **H₂** at 650 nm; b) emission from **Zn₂1** at 650 nm; c) emission from a 2:1 mixture of **Zn₂1** and **H₂**.

decay time for **H₂2** is 9500 ± 100 ps. For the 2:1 complex, the zinc porphyrin was preferentially excited at 562 nm, and the decay of the excited state monitored at 600 nm where only the zinc porphyrins emit was nonexponential. A simple model which assumes there are two independent processes for deactivation of the zinc porphyrin excited state, fluorescence (with a lifetime of 1330 ps as observed for **Zn₂1**) and energy transfer, fits the fast part of the decay well and gives an energy-transfer time of 490 ps. The intensity of the 720 nm emission from **H₂2** was too weak to extract reliable kinetic parameters for the increase in fluorescence.^[17] Thus the rate of the energy-transfer process illustrated in Scheme 1 is 2×10^9 s⁻¹. These rate constants give a quantum yield for energy transfer of 73 %, which is in good agreement with the steady-state experiments.^[18]

In conclusion, self-assembly offers a relatively straightforward method for the construction of large multi-chromophore arrays with extremely well-defined three-dimensional structures. The system described here functions as a simple light-harvesting antennae system which funnels incident excitation energy into the center of the complex, but other more sophisticated arrangements may be envisaged.

Received: May 12, 2000 [Z15118]

- [1] a) S. M. Prince, M. Z. Papiz, A. A. Freer, G. McDermott, A. M. Hawthornwaite-Lawless, R. J. Cogdell, N. W. Isaacs, *J. Mol. Biol.* **1997**, *268*, 412–423; b) G. McDermott, S. M. Prince, A. A. Freer, A. M. Hawthornwaite-Lawless, M. Z. Papiz, R. J. Cogdell, N. W. Isaacs, *Nature* **1995**, *374*, 517–521.
- [2] J. Dissenhofer, O. Epp, K. Miki, R. Huber, H. Michel, *Nature* **1985**, *318*, 618–624.
- [3] G. Feher, J. P. Allen, M. Y. Okamura, D. C. Rees, *Nature* **1989**, *339*, 111–116.
- [4] R. Van Grondelle, J. P. Dekker, T. Gillbro, V. Sundström, *Biochim. Biophys. Acta* **1994**, *1187*, 1–65.
- [5] T. Pullerits, V. Sundström, *Acc. Chem. Res.* **1996**, *29*, 381–389.
- [6] a) A. Harriman, *Supramolecular Photochemistry*, (Ed.: V. Balzani), Reidel, Dordrecht, **1987**, pp. 207–238; b) J. K. M. Sanders in *Comprehensive Supramolecular Chemistry*, Vol. 9 (Ed.: J. L. Atwood), Pergamon, Oxford, **1997**, pp. 131–164.
- [7] a) J. Seth, V. Palaniappan, T. E. Johnson, S. Prathapan, J. S. Lindsey, D. E. Bocian, *J. Am. Chem. Soc.* **1994**, *116*, 10578–10592; b) J. Z. Li, A. Ambroise, S. I. Yang, J. R. Diers, J. Seth, C. R. Wack, D. F. Bocian, D. Holten, J. S. Lindsey, *J. Am. Chem. Soc.* **1999**, *121*, 8927–8940; c) D. Kuciauskas, P. A. Liddell, S. Lin, T. E. Johnson, S. J. Weghorn, J. S. Lindsey, A. L. Moore, T. A. Moore, D. Gust, *J. Am. Chem. Soc.* **1999**, *121*, 8604–8614.
- [8] a) T. Nagata, A. Osuka, K. Marayuma, *J. Am. Chem. Soc.* **1990**, *112*, 3054–3059; b) A. Nakano, A. Osuka, I. Yamazaki, T. Yamazaki, Y. Nishimura, *Angew. Chem.* **1998**, *110*, 3172–3176; *Angew. Chem. Int. Ed.* **1998**, *37*, 3023–3027.
- [9] H. A. M. Biemans, A. E. Rowan, A. Verhoeven, P. Vanoppen, L. Latterini, J. Foekema, A. P. H. Schenning, E. W. Meijer, F. C. de Schryver, R. J. M. Nolte, *J. Am. Chem. Soc.* **1998**, *120*, 11054–11060.
- [10] P. N. Taylor, H. L. Anderson, *J. Am. Chem. Soc.* **1999**, *121*, 11538–11545.
- [11] a) S. Anderson, H. L. Anderson, J. K. M. Sanders, *Acc. Chem. Res.* **1993**, *26*, 469–475; b) S. Anderson, H. L. Anderson, A. Bashall, M. McPartlin, J. K. M. Sanders, *Angew. Chem.* **1995**, *107*, 1196; *Angew. Chem. Int. Ed. Engl.* **1995**, *34*, 1096–1099.
- [12] a) C. A. Hunter, L. D. Sarson, *Angew. Chem.* **1994**, *106*, 2424–2427; *Angew. Chem. Int. Ed. Engl.* **1994**, *33*, 2313–2316; b) X. Chi, A. J. Guerin, R. A. Haycock, C. A. Hunter, L. D. Sarson, *J. Chem. Soc. Chem. Commun.* **1995**, 2567–2569; c) C. A. Hunter, R. H. Hyde, *Angew. Chem.* **1996**, *108*, 2064–2067; *Angew. Chem. Int. Ed. Engl.* **1996**, *35*, 1936–1939.
- [13] A related architecture was reported by J. N. H. Reek, A. P. H. Schenning, A. W. Bosman, E. W. Meijer, M. J. Crossley, *Chem. Commun.* **1998**, 11–12.
- [14] The porphyrin *meso* substituents are depicted in an $\alpha\beta\alpha\beta$ conformation, but exchange between different atropisomers is fast (on the seconds timescale), and so they equilibrate rapidly to the most stable arrangement for complexation. Models suggest that while **Zn₂1** could coordinate across two *cis-meso* ligands, this arrangement is less favorable than the *trans* structure shown in Scheme 1.
- [15] J. S. Lindsey, R. W. Wagner, *J. Org. Chem.* **1989**, *54*, 828–836.
- [16] We used racemic 2-ethylhexyl substituents to solubilize **H₂2**, so the compound is actually a mixture of diastereoisomers. However, the chiral centers are sufficiently far away from the sites of interaction that no adverse consequences are observed, and the solubility of the porphyrin is dramatically improved. We have also prepared a diastereomeric mixture of the 2-ethylhexyl analogue of **Zn₂1**, and the behavior of this system is identical to the *n*-pentyl-solubilized compound. **Zn₂1**: ¹H NMR (250 MHz, CDCl₃): δ = 1.0 (102 H, m), 1.50 (132 H, m), 1.80 (6 H, quin), 1.90 (6 H, quin), 3.95 (12 H, d), 4.15 (12 H, d), 7.20 (6 H, d), 7.70 (6 H, d), 7.75 (6 H, s), 8.30 (8 H, m), 8.75 (3 H, d), 9.05 (16 H, m), 10.00 (2 H, s); MS (+ve FAB) *m/z* calcd for C₁₉₁H₂₅₁N₁₁O₁₄Zn: 3055.91; found: 3057 [MH⁺]; elemental analysis calculated for C₁₉₁H₂₅₁N₁₁O₁₄Zn: C 75.07, H 8.28, N 5.04%; found: C 75.03, H 8.26, N 4.84%; m.p. 235–237 °C; λ_{max} (ϵ): 425.6 (7.52×10^5), 550.4 (4.97×10^4), 590.4 nm (1.72×10^4). **H₂2**: ¹H NMR (250 MHz, CDCl₃): δ = 2.75 (2 H, s), 1.00 (36 H, m), 1.50 (44 H, m), 2.00 (4 H, quin), 4.25 (8 H, d), 7.35 (4 H, d), 7.8 (8 H, d), 7.90 (4 H, dd), 8.80 (8 H, d), 9.0 (12 H, s), 9.45 (4 H, m); MS (+ve FAB) *m/z* calcd for C₁₀₀H₁₁₀N₁₂O₈: 1608.04; found: 1608 [M⁺]; accurate mass (+ve FAB) calculated mass for C₁₀₀H₁₁₀N₁₂O₈: 1607.864785; found: 1607.857164 (+7.6 mDa, +4.7 ppm). Elemental analysis calcd for C₁₀₀H₁₁₀N₁₂O₈·H₂O: C 73.84, H 6.94, N 10.33%; found C 73.94, H 6.89, N 10.48%; m.p. > 298 °C; λ_{max} (ϵ): 424.5 (3.39×10^5), 519.0 (1.82×10^4), 556.0 (1.14×10^4), 593.0 (6.10×10^3), 649.0 nm (5.50×10^3). **Zn3**: ¹H NMR (250 MHz, CDCl₃): δ = 8.95 (8 H, s), 7.80 (4 H, s), 7.70 (4 H, d), 7.23 (4 H, d), 4.20 (8 H, d), 4.00 (8 H, d), 1.2–2.1 (64 H, m), 0.8–1.19 (48 H, m); MS (+ve FAB) *m/z* calcd for C₁₀₈H₁₅₆N₄O₈Zn: 1703.44; found: 1703 [M⁺]; m.p. 141.8 °C; λ_{max} (ϵ): 426.0 (2.30×10^5), 553.0 (2.20×10^4), 594.0 nm (7.05×10^4).
- [17] The emission from **H₂2** at 720 nm is complicated by the dynamics in the red wing of the decaying fluorescence of **Zn₂1**. Qualitatively, there was a rise component in the fluorescence at 720 nm, which is consistent with the 500 ps time scale determined from the decay in the signal at 600 nm, but the fluorescence of **H₂2** at 720 nm was too weak relative to the intense **Zn₂1** fluorescence to extract reliable kinetic parameters.
- [18] Quantum yield of energy transfer = $k(\text{energy transfer})/[k(\text{energy transfer}) + k(\text{fluorescence})]$.